

# Stereospecific and Kinetic Control over the Hydrolysis of a Sterically Hindered Platinum Picoline Anticancer Complex

Yu Chen, Zijian Guo, Simon Parsons, and Peter J. Sadler\*

**Abstract:** *cis*-[PtCl<sub>2</sub>(NH<sub>3</sub>)(2-picoline)] (**1**) (AMD473) is a recently reported active anticancer complex. Hydrolysis may be an important step in its intracellular activation and interaction with DNA. In this paper we employed [<sup>1</sup>H, <sup>15</sup>N] 2D NMR spectroscopy to determine the hydrolysis rates for each chloride ligand of this complex and its 3-picoline analogue **2**. We also report the p*K*<sub>a</sub> values of the aqua and diaqua ligands as well as the X-ray crystal structures of **1** and **2**. For the 3-picoline complex **2** the rate of hydrolysis of the Cl<sup>-</sup> *trans* to NH<sub>3</sub> (*k*<sub>1b</sub> = 1.0 × 10<sup>-4</sup> s<sup>-1</sup>, *I* = 0.1M, 310 K) is similar to that of cisplatin, but slower for the Cl<sup>-</sup> *trans* to 3-picoline (*k*<sub>1a</sub> = 4.5 × 10<sup>-5</sup> s<sup>-1</sup>). Both of

the first hydrolysis rates for the 2-picoline complex **1** are slower than those of **2**, but in contrast to **2**, the hydrolysis of the Cl<sup>-</sup> *trans* to NH<sub>3</sub> (*cis* to 2-picoline) is slower (*k*<sub>1b</sub> = 2.2 × 10<sup>-5</sup> s<sup>-1</sup>) than for the Cl<sup>-</sup> *trans* to 2-picoline (*k*<sub>1a</sub> = 3.2 × 10<sup>-5</sup> s<sup>-1</sup>). The crystal structure of **2** revealed that the pyridine ring is tilted by 49° with respect to the Pt square plane, whereas in **1** the ring is almost perpendicular (103°). This introduces steric hindrance by the CH<sub>3</sub> group towards an axial approach to Pt from

above, leading to a destabilisation of the expected trigonal-bipyramidal transition state, an effect well-known in substitution reactions of Pt<sup>II</sup> complexes. The p*K*<sub>a</sub> values for the mono aqua adducts of **1** (6.13 and 6.49) and **2** (5.98 and 6.26 for H<sub>2</sub>O *trans* to picoline and NH<sub>3</sub>, respectively) and for the diaqua adducts (5.22, 7.16 for **1** and 5.07, 6.94 for **2**) are >0.3 units lower than for cisplatin. The slowness of the hydrolysis, combined with the dominance of (inert) hydroxo species, is expected to contribute to a greatly reduced reactivity of the sterically hindered 2-picoline complex under intracellular conditions.

**Keywords:** antitumor agents • bioinorganic chemistry • hydrolysis • platinum • structure elucidation

## Introduction

Cisplatin is a widely used anticancer drug; however, there is a need for new agents which do not exhibit cross-resistance and which are less toxic.<sup>[1]</sup> Most of the active platinum compounds have the general formula *cis*-[PtAm<sub>2</sub>X<sub>2</sub>], where Am is an am(m)ine ligand with at least one NH group and X is a moderately strongly bound anionic leaving group, such as chloride.<sup>[2]</sup> Recently, there has been interest in pyridine complexes.<sup>[3–5]</sup> The presence of planar pyridine ligands, as in *cis* or *trans*-[PtCl<sub>2</sub>(pyridine)<sub>2</sub>] complexes, can reduce the rates of DNA binding compared to *cis* and *trans*-DDP,<sup>[6]</sup> and by changing the nature or position of substituents on the pyridine ligands, different binding affinities for DNA can be achieved.<sup>[4]</sup>

The 2-picoline (2-methylpyridine) complex *cis*-[PtCl<sub>2</sub>(NH<sub>3</sub>)(2-picoline)] (**1**) (AMD473), a recently reported anticancer complex, has now entered clinical trials.<sup>[7]</sup> It is reported to

possess activity against cisplatin-resistant cell lines, and against a subline of a human ovarian carcinoma xenograph with acquired cisplatin resistance, by injection and oral administration. No chemical studies of the complex have been reported, although it appears to form interstrand DNA cross-links and to bind to plasma proteins much more slowly than cisplatin.<sup>[8]</sup> For this report we have labelled complex **1** with <sup>15</sup>N and compared its hydrolysis behaviour with that of the isomeric 3-picoline derivative **2**, since hydrolysis is likely to be an important initial activation step for this drug. We have also determined the p*K*<sub>a</sub> values for the mono and diaqua complexes, since hydroxo ligands on Pt<sup>II</sup> are usually inert compared to aqua ligands. The data reveal notable differences between the chemistry of the sterically hindered picoline complex and that of cisplatin.

## Experimental Section

**Chemicals and preparation of complexes:** 2- and 3-Picoline were purchased from Aldrich. *Cis*-[PtCl<sub>2</sub>(<sup>15</sup>NH<sub>3</sub>)<sub>2</sub>] was prepared according to a reported procedure.<sup>[9]</sup> Complexes **1** and **2** were prepared by a procedure similar to that described in the literature for natural-abundance, mixed ligand ammine/amine Pt<sup>II</sup> complexes.<sup>[10]</sup>

[\*] Prof. Dr. P. J. Sadler, Y. Chen, Dr. Z. Guo, Dr. S. Parsons  
Department of Chemistry, University of Edinburgh  
West Mains Road, Edinburgh EH9 3JJ (UK)  
Fax: (+ 44) 131-650-6452  
E-mail: p.j.sadler@ed.ac.uk

**Complex 1:**  $^1\text{H NMR}$ :  $\delta = 8.87$  (d,  $J = 8$  Hz, 1H, H6), 7.81 (m, 1H, H4), 7.49 (d,  $J = 8$  Hz, 1H, H3), 7.32 (m, 1H, H5), 3.13 (s, 3H,  $\text{CH}_3$ ); Anal. calcd for  $\text{C}_6\text{H}_{10}\text{Cl}_2\text{N}^{15}\text{Npt}$ : C 19.1, H 2.65, N 7.69; found: C 19.28, H 2.97, N 7.57.

**Complex 2:**  $^1\text{H NMR}$ :  $\delta = 8.62$  (s, 1H, H2), 8.54 (d,  $J = 6$  Hz, 1H, H6), 7.77 (d,  $J = 9$  Hz, 1H, H4), 7.37 (m, 1H, H5), 2.35 (s, 3H,  $\text{CH}_3$ ); Anal. found: C 18.82, H 2.70, N 7.31

**pH Measurements:** These were performed with a Corning 145 pH meter equipped with an Aldrich micro combination electrode calibrated with Aldrich buffer solutions of pH 4, 7 and 10. The values of the pH were adjusted with 1M  $\text{HClO}_4$  or NaOH as appropriate.

**X-ray crystallography:** Crystals of complexes **1** ( $^{15}\text{NH}_3$ ) and **2** ( $^{14}\text{NH}_3$ ) were obtained by the slow evaporation of aqueous solutions containing excess KCl. Data for **1** and **2** were collected on a Stadi-4 diffractometer equipped with an Oxford Cryosystems low-temperature device. Scan modes were both  $\omega - \theta$ . Complex **2** crystallised as fine delicate needles, which tended to form coaxially aligned clumps and exhibited broad diffraction profiles. For these reasons,  $\text{Cu}_{\text{K}\alpha}$  radiation was used for its greater intensity than  $\text{Mo}_{\text{K}\alpha}$  radiation. The structures were refined by full-matrix least-squares against  $F^2$  (SHELXL 1). H atoms were placed in calculated positions; the  $\text{CH}_3$  and  $\text{NH}_3$  were modelled as rotating rigid groups. All non-H atoms were refined anisotropically.

Crystal data for the two structures are listed in Table 1, and selected bond lengths and angles are given in Table 2. Crystallographic data (excluding structure factors) for the structures reported in this paper have been

Table 1. Crystal structure data for complexes **1** and **2**.

	<b>1</b>	<b>2</b>
empirical formula	$\text{C}_6\text{H}_{10}\text{Cl}_2\text{N}^{15}\text{Npt}$	$\text{C}_6\text{H}_{10}\text{Cl}_2\text{N}_2\text{Pt}$
$M_r$	377.1	376.1
colour	yellow	yellow
crystal size (mm)	$0.47 \times 0.39 \times 0.25$	$0.43 \times 0.08 \times 0.08$
crystal shape	block	needle
crystal system	monoclinic	orthorhombic
space group	$P2_1/c$	$Pbca$
$a$ (Å)	9.859(2)	12.287(8)
$b$ (Å)	8.910(2)	7.318(8)
$c$ (Å)	11.197(2)	20.801(14)
$\beta$ (°)	102.684(15)	90
$V$ (Å <sup>3</sup> )	959.6(3)	1871(3)
$Z$	4	8
$\lambda$ (Å)	0.71073	1.54178
$T$ (K)	220(2)	220(2)
$\rho_{\text{calcd}}$ (g cm <sup>-3</sup> )	2.604	2.420
$\mu_{\text{calcd}}$ (mm <sup>-1</sup> )	15.119 ( $\text{Mo}_{\text{K}\alpha}$ )	30.166 ( $\text{Cu}_{\text{K}\alpha}$ )
$F(000)$	688	1240
$2\theta$ range (°)	5.9–50	8.5–140
abs. correction ( $T_{\text{min/max}}$ )	$\Psi$ -scans (0.0033/0.0175)	Shelxa (0.0263/0.4036)
refl. collected	3725	4662
unique refl.	1688 ( $R_{\text{int}} = 0.0358$ )	1672 ( $R_{\text{int}} = 0.0560$ )
refl. used	1684	1670
parameters	102	101
$R1$ ( $F_0 > 4\sigma(F_0)$ ) <sup>[a]</sup>	0.0355	0.0437
$wR2$ (all data) <sup>[b]</sup>	0.0903	0.1183
$g1$ ; $g2$ <sup>[c]</sup>	0.0596; 0.0000	0.0746; 0.0000
resid. elec. density (e Å <sup>-3</sup> )	+1.52/–1.16	+1.56/–2.72

[a]  $R1 = \Sigma(|F_o| - |F_c|)/\Sigma|F_o|$ . [b]  $wR2 = \{\Sigma[w(F_o^2 - F_c^2)^2]/\Sigma[w(F_o^2)]\}^{1/2}$ . [c]  $w = 1/[\sigma^2(F_o^2) + (g1 \times P)^2 + g2 \times P]$ ;  $P = (F_o^2 + 2F_c^2)/3$ .

deposited with the Cambridge Crystallographic Data Centre as supplementary publication no. CCDC-100573. Copies of the data can be obtained free of charge on application to CCDC, 12 Union Road, Cambridge CB2 1EZ, UK (Fax: (+ 44)1223-336-033; e-mail: deposit@ccdc.cam.ac.uk).

**NMR spectroscopy:** NMR spectra were recorded on a Bruker DMX 500 instrument in 5 mm tubes. All the samples were recorded in 90%  $\text{H}_2\text{O}/10\%$   $\text{D}_2\text{O}$  (0.6 mL) containing 0.1M  $\text{NaClO}_4$  to maintain a constant ionic

Table 2. Selected bond lengths (Å) and angles (°) for complexes **1** and **2**.

	<b>1</b>	<b>2</b>
Pt–N(1)	2.017(8)	2.008(8)
Pt–N(2)	2.030(8)	2.039(9)
Pt–Cl(1)	2.299(2)	2.296(3)
Pt–Cl(2)	2.322(2)	2.309(3)
N(1)–Pt–N(2)	90.5(3)	90.5(4)
N(1)–Pt–Cl(1)	177.6(2)	177.3(3)
N(2)–Pt–Cl(1)	87.3(2)	86.8(3)
N(1)–Pt–Cl(2)	89.5(2)	90.9(2)
N(2)–Pt–Cl(2)	176.1(3)	178.6(3)
Cl(1)–Pt–Cl(2)	92.70(8)	91.72(10)

strength. The chemical shifts are reported relative to sodium trimethylsilyl[ $\text{D}_4$ ]propionate (through internal dioxane at  $\delta = 3.743$ ) for  $^1\text{H}$ , and 1M  $^{15}\text{NH}_4\text{Cl}$  in 1.5M HCl for  $^{15}\text{N}$  (external). Typical acquisition conditions for  $^1\text{H}$  spectra were: 45–60° pulses, 2.5 s relaxation delay, 64–256 transients, final digital resolution 0.2 Hz per point. When necessary, the water resonance was suppressed by presaturation, or by means of the WATERGATE pulsed-field-gradient sequence.<sup>[11]</sup>

Both 1D  $^{15}\text{N}$ -edited  $^1\text{H}$  NMR spectra and 2D [ $^1\text{H}$ ,  $^{15}\text{N}$ ] heteronuclear single-quantum coherence (HSQC) spectra (optimised for  $^1J(\text{N,H}) = 72$  Hz) were recorded with the use of the sequence of Stonehouse et al.<sup>[12]</sup> The  $^{15}\text{N}$  spins were decoupled by irradiating with the GARP-1 sequence during acquisition.

**Data analysis:** For the kinetic analysis of NMR data, the appropriate differential equations were integrated numerically, and the rate constants were determined by a nonlinear optimisation procedure by the programme SCIENTIST (Version 2.01, MicroMath). The errors represent one standard deviation. Equilibrium constants were calculated from the equilibrium concentrations of species determined by integration of the 2D spectra.

Titration curves were fitted to the Henderson–Hasselbalch equation using the programme KaleidaGraph (Synergy Software, Reading, PA, USA) on a Macintosh computer.

## Results and Discussion

**X-ray crystal structures:** We first prepared both natural-abundance and  $^{15}\text{N}$ -labeled complexes **1** and **2** and crystallised them for X-ray analysis. Both have a square-planar configuration with angles close to the ideal values of 90° and 180° (Figure 1). In complex **1**, the Pt–Cl(2) bond *trans* to  $\text{NH}_3$  is

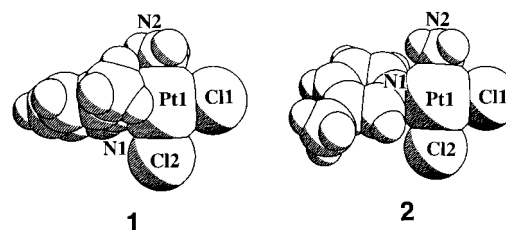


Figure 1. X-ray crystal structures of complexes **1** and **2** illustrating the steric hindrance caused by the 2-methyl group in complex **1**.

slightly longer (2.322(2) Å) than normal, while the Pt–Cl(1) bond length (2.299(2) Å) is within the normal range. In complex **2** both Pt–Cl bond lengths (2.296(3) Å, 2.309(3) Å) are close to the expected values. The Pt–N(1) bond lengths in both complex **1** (2.017(8) Å) and **2** (2.008(8) Å) are comparable to those of *cis*-[Pt(py)<sub>2</sub>Cl<sub>2</sub>] (2.01 and 2.04 Å).<sup>[13]</sup> The most notable feature of the structures is the orientation of the

picoline ring with respect to the Pt square plane. The 3-picoline ligand is tilted by  $48.9^\circ$ , whereas the 2-picoline ligand is almost perpendicular ( $102.7^\circ$ ) to the plane, so that the 2-methyl group lies directly over the square plane ( $\text{H}_3\text{C}\cdots\text{Pt}$ : 3.224 Å). The space-filling model (Figure 1) demonstrates that this introduces steric hindrance to an axial approach to Pt from above. The steric effect leads to a slight twisting of the  $[\text{PtN}_2\text{Cl}_2]$  square plane, with a mean deviation of the atoms from the plane of 0.0406 Å, which is an order of magnitude higher than that for complex **2**.

There are strong intermolecular hydrogen bonds involved in the crystal packing of both complexes (Figure 2). For complex **1**, the three H atoms of the  $\text{NH}_3$  ligand are H-bonded to four Cl ligands from two neighbouring molecules, while for complex **2**, H-bonds of similar strength are formed only to three of the four Cl ligands. Such intermolecular H bonds are common in chloro  $\text{Pt}^{\text{II}}$  am(m)ine complexes.<sup>[14, 15]</sup> A very weak, graphitic type of interaction between the picoline groups of neighbouring molecules of **1** may also be present. In complex **1**, layers containing  $\text{Cl}\cdots\text{H}-\text{N}$  H-bonding interactions alternate with layers containing picoline groups. In complex **2**, the molecules themselves form layers, with H bonds both within and between layers.

**Hydrolysis:** The  $^1\text{H}$ ,  $^{15}\text{N}$  2D NMR spectra of  $^{15}\text{NH}_3$ -labelled **1** and **2** in aqueous solutions containing 0.1M  $\text{NaClO}_4$  were each monitored for a period of over 20 h at 310 K. Initially, a single cross-peak was observed at  $\delta = 4.15/-66.52$ , which was assigned to the dichloro complex **1**. After 1 h, two additional cross-peaks with similar intensities were detected at  $\delta = 4.40/-64.41$  and  $4.32/-87.25$ . The former peak is consistent with an assignment to complex **3a**, with an  $^{15}\text{N}$  shift diagnostic of  $^{15}\text{N}$  *trans* to N or Cl,<sup>[16]</sup> and the latter to **3b** with  $^{15}\text{N}$  *trans* to O, Scheme 1. Both peaks increased in intensity for several hours, while the peak for **1** decreased in intensity. After about 2.5 h, a

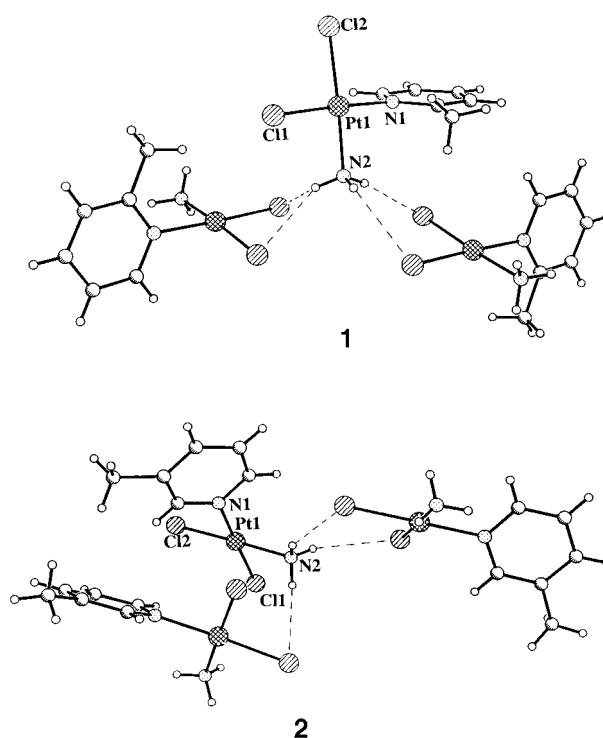
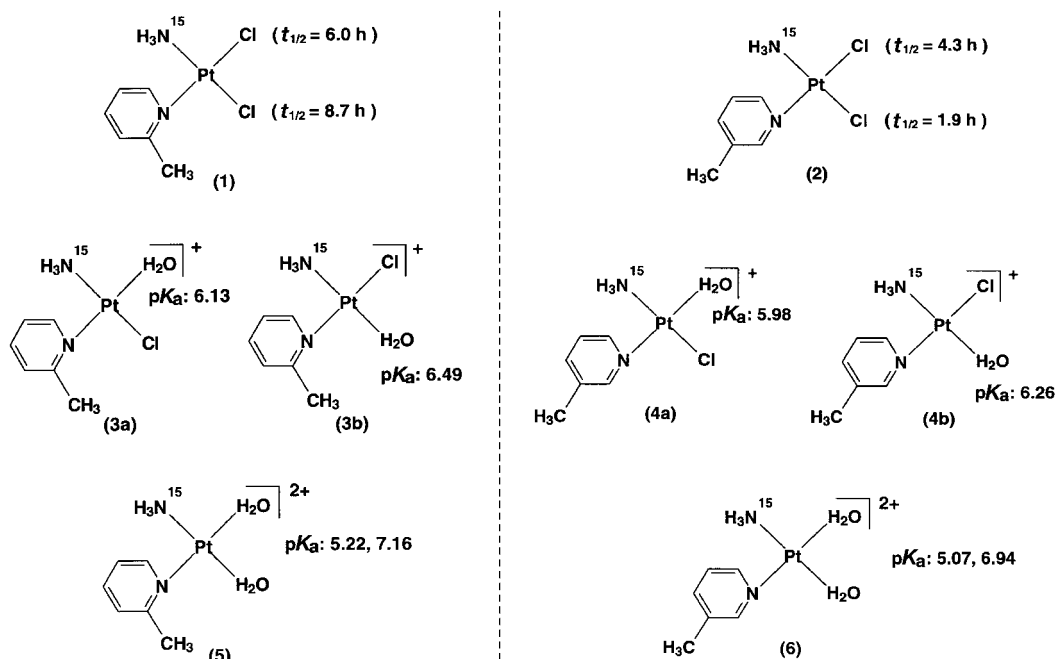


Figure 2. Intermolecular hydrogen bonding in crystals of complexes **1** and **2**;  $\text{N}-\text{H}\cdots\text{Cl}$  distances for complex **1** range from 2.55 Å to 2.74 Å and for complex **2** from 2.62 Å to 2.81 Å.

fourth cross-peak appeared at  $\delta = 4.41/-82.91$ . This was assigned to the diaqua complex **5** (Figure 3 A); however, even after 20 h, this accounted for only  $<10\%$  of the total  $^{15}\text{NH}_3$ -Pt species present.

For the 3-picoline complex **2**, the time-dependence of the  $^1\text{H}$ ,  $^{15}\text{N}$  2D NMR spectrum was similar to that of complex **1**, except that the cross-peak **c** (Figure 3 B), assigned to one of



Scheme 1. Comparison of half-lives for the hydrolysis (310 K) and  $\text{pK}_a$  values (298 K) of platinum-picoline complexes (0.1M  $\text{NaClO}_4$ ).

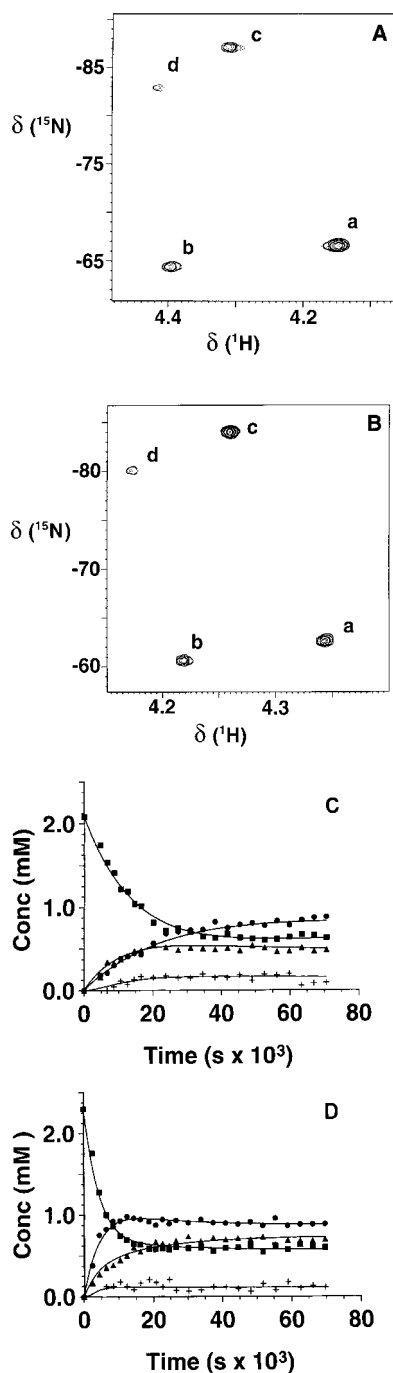


Figure 3. 2D [ $^1\text{H}$ ,  $^{15}\text{N}$ ] HSQC NMR spectra of 3 mM aqueous solutions of: A)  $\text{cis-}[\text{PtCl}_2(^{15}\text{NH}_3)(2\text{-picoline})]$  (**1**) and B)  $\text{cis-}[\text{PtCl}_2(^{15}\text{NH}_3)(3\text{-picoline})]$  (**2**) after 3 h at 310 K. Peak **a** is assigned to the starting complex, peaks **b**, **c** to the two mono-aqua complexes ( $\text{H}_2\text{O}$  *cis* to  $\text{NH}_3$  and  $\text{H}_2\text{O}$  *trans* to  $\text{NH}_3$ , respectively), and peak **d** to the diaqua complex. Time dependence of the concentrations of the dichloro and aqua adducts of C) **1** and D) **2**. Labels: **1** and **2** ( $\blacksquare$ ), mono-aqua complexes **3a** and **4a** ( $\blacktriangle$ ), mono-aqua complexes **3b** and **4b** ( $\bullet$ ), diaqua complexes **5** and **6** ( $+$ ). The curves are the best fits calculated with the rate constants shown in Table 3.

the two mono-aqua complexes, was more intense than the other. The  $^{15}\text{N}$  chemical shifts for the peaks of the 3-picoline complexes are shifted slightly to lower field with respect to those of the 2-picoline adducts. However, the  $^1\text{H}$  chemical shifts are very similar. The time-dependence of the concen-

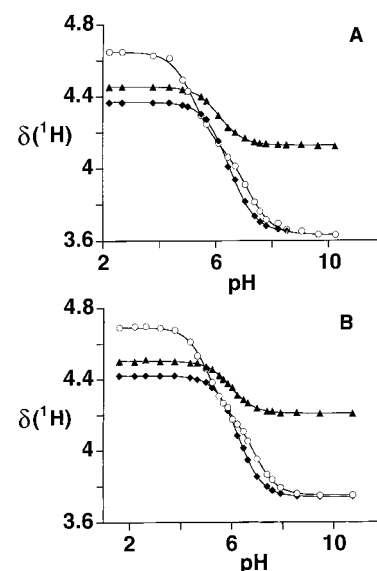


Figure 4. pH-dependence of the  $^1\text{H}$  NMR chemical shifts of  $\text{NH}_3$  in the mono-aqua and diaqua complexes: A) complex **1**, and B) complex **2**. The curves represent best fits calculated with the  $\text{p}K_a$  values listed in Scheme 1. Labels: mono-aqua complexes **3a** and **4a** ( $\blacktriangle$ ), mono-aqua complexes **3b** and **4b** ( $\bullet$ ), diaqua complexes **5** and **6** ( $\circ$ ).

trations of species detected during hydrolysis of complexes **1** and **2** is shown in Figures 3 C and 3 D. The assignments of the peaks for the aqua complexes were confirmed by pH titrations (Figure 4), and these allowed the determination of the  $\text{p}K_a$  value for each mono-aqua complex, as well as two  $\text{p}K_a$  values for each diaqua complex (Scheme 1).

The NMR data allow the determination of the hydrolysis rates for each individual chloride ligand in the initial complexes **1** and **2**, and in the mono-aqua complexes **3a**, **b** and **4a**, **b** (Table 3). It is notable that the hydrolysis rates of the two  $\text{Cl}^-$  ligands of complex **1** are both slower than those for complex **2** (Table 3). The  $\text{Cl}^-$  ligand *trans* to  $\text{NH}_3$  in complex **1** hydrolyses about four times more slowly than that in the unhindered complex **2**. In complex **2**, the  $\text{Cl}^-$  ligand *trans* to  $\text{NH}_3$  hydrolyses about twice as fast as that *trans* to 3-picoline. This might be expected from the higher *trans* influence of  $\text{NH}_3$  ( $\text{p}K_a = 9.29$ )<sup>[17]</sup> versus 3-picoline ( $\text{p}K_a = 6.0$ )<sup>[17]</sup> However, for complex **1**, the situation is reversed: hydrolysis is faster for the  $\text{Cl}^-$  ligand *trans* to 2-picoline ( $\text{p}K_a = 6.1$ )<sup>[17]</sup> All the first-step hydrolysis rates determined here are slower than that of cisplatin ( $t_{1/2}$ : 1.75 h at 310 K).<sup>[18]</sup>

Axial steric interactions have long been known to decrease the rate of substitution reactions of square-planar complexes.<sup>[19]</sup> For example, the rate of reaction of 2-picoline with  $[\text{AuCl}_4]^-$  is about 9 times slower than with 3-picoline, but 10 times faster than with 2,6-dimethylpyridine, which blocks both axial sites. In the complexes  $\text{cis-}[\text{Pt}(\text{PEt}_3)_2(\text{R})\text{Br}]$ , the rate of displacement of  $\text{Br}^-$  by  $\text{MeOH}$  decreases dramatically as the steric hindrance by the aryl ligand R, which is *cis* to the leaving group, increases:  $\text{Ph} \approx p\text{-MeC}_6\text{H}_4 \gg o\text{-MeC}_6\text{H}_4 > o\text{-EtC}_6\text{H}_4 > 2,4,6\text{-Me}_3\text{C}_6\text{H}_2$ .<sup>[20]</sup> In an associative mechanism with a trigonal-bipyramidal transition state, the ligands *cis* to the leaving group become axial to the trigonal plane in the 5-coordinate transition state, and interact with the entering and leaving groups at an angle of  $90^\circ$ , so that the steric effect is

Table 3. Rate and equilibrium constants for the hydrolysis of the platinum–picoline complexes **1** (pH=4.6) and **2** (pH=4.4) at 310 K (0.1M NaClO<sub>4</sub>). Data reported for cisplatin under related conditions (308 K, 0.32M KNO<sub>3</sub>) are listed for comparison.

	Rate constants <sup>[a]</sup> (10 <sup>-6</sup> s <sup>-1</sup> )	Equilibrium constants <sup>[b]</sup> (10 <sup>-4</sup> M)
<b>1</b>	$k_{1a}$ : 31.9 ± 1.5	$K_{1a}$ : 12.1
2-picoline	$k_{1b}$ : 22.1 ± 1.4	$K_{1b}$ : 21.4
	$k_{2a}$ : 73 ± 14	$K_{2a}$ : 4.8
	$k_{2b}$ : 3.5 ± 2.5	$K_{2b}$ : 2.7
<b>2</b>	$k_{1a}$ : 44.7 ± 1.9	$K_{1a}$ : 23.2
3-picoline	$k_{1b}$ : 103 ± 4	$K_{1b}$ : 28.0
	$k_{2a}$ : 35.0 ± 1.7	$K_{2a}$ : 2.8
	$k_{2b}$ : 78 ± 60	$K_{2b}$ : 2.3
cisplatin <sup>[c]</sup>	$k_1$ : 75.9	$K_1$ : 43.7

[a] The errors in the rates for the second hydrolysis step are large because the fitting process is relatively insensitive to the rate of the back reaction. Therefore, these constants are not discussed in the text. [b] Constants correspond to kinetic steps indicated, that is  $K_{1a}$  to equilibrium between **1** (or **2**) and **3a** (or **4a**), etc. [c] Ref. [18].

more prominent on the ligand in the position *cis* to the bulky ligand.

**pK<sub>a</sub> values:** A change of the methyl group from the 2- to the 3-position only has a small effect on the pK<sub>a</sub> values of the aqua ligands, lowering them by about 0.2 units (Scheme 1). The pK<sub>a</sub> values for both the mono-aqua and diaqua adducts of the 2-picoline and 3-picoline complexes are >0.3 units lower than that of cisplatin. This means that although the sterically hindered 2-picoline complex **1** will exist predominantly (about 70%) as a dichloro adduct under extracellular conditions (0.1M Cl<sup>-</sup>, pH 7.4), under intracellular conditions (4 mM Cl<sup>-</sup>, pH 7.4), the hydroxo/chloro and dihydroxo adducts of **1** will predominate (>70%), whereas for cisplatin the dichloro, chloro/aqua and chloro/hydroxo are present in about equal proportions (about 30% each).<sup>[21]</sup> The slowness of the hydrolysis steps of complex **1** (Table 3) coupled with the dominance of (inert) hydroxo species would both be expected to contribute to its greatly reduced reactivity under intracellular conditions.

## Conclusions

The Cl<sup>-</sup> ligand *cis* to 2-picoline (*trans* to NH<sub>3</sub>) in the complex *cis*-[PtCl<sub>2</sub>(NH<sub>3</sub>)(2-picoline)] (**1**) hydrolyses about 4 times more slowly than that in cisplatin ( $t_{1/2}$ : 8.7 h at 310 K, compared with 1.8 h for cisplatin), and both Cl<sup>-</sup> ligands of **1**

hydrolyse more slowly than the 3-picoline analogue **2**. X-ray crystallography has confirmed the steric hindrance introduced by the 2-methyl group of the picoline ligand in **1**. This hindrance has the effect of destabilising the expected trigonal-bipyramidal transition state, an effect well-known in substitution reactions of square-planar Pt<sup>II</sup> complexes.<sup>[19]</sup> The pK<sub>a</sub> values of the mono-aqua and diaqua adducts of both **1** and **2** are >0.3 units lower than those similar cisplatin adducts. This, combined with slower hydrolysis (Table 3), is likely to result in a reduced intracellular activity of complex **1** compared to cisplatin and may contribute to its high activity against cisplatin-resistant cell lines. Our preliminary studies of reactions of complexes **1** and **2** with guanosine 5'-monophosphate (5'-GMP) have established that hydrolysis is the rate-limiting step for both complexes **1** and **2**. The formation of the bis-GMP adduct of complex **1** is about twice as slow as that for complex **2**, which is consistent with the brief report that complex **1** forms DNA cross-links extremely slowly.<sup>[8]</sup> Further NMR studies should allow detailed insight to be gained into the effect of steric hindrance on the formation of DNA adducts.

**Acknowledgments:** This research was supported by the Biotechnology and Biological Sciences Research Council, Engineering and Physical Sciences Research Council (Biomolecular Sciences Programme), and ECCOST programme. We are grateful to Dr. J. A. Parkinson for advice on NMR measurements, the CVCP for an ORS Award and University of Edinburgh for a Research Studentship for Y. Chen, Johnson Matthey for the loan of some platinum, and Dr. B. Murrer (Johnson Matthey) for helpful discussions.

Received: October 7, 1997 [F845]

- [1] *Platinum and Other Metal Coordination Compounds in Cancer Chemotherapy 2* (Eds.: H. M. Pinedo, J. H. Schornagel), Plenum, New York, 1996.
- [2] J. Reedijk, *Chem. Commun.* 1996, 801.
- [3] M. Vanbeusichem, N. Farrell, *Inorg. Chem.* 1992, 31, 634.
- [4] M. Cusumano, M. L. Di Pietro, A. Giannetto, *Chem. Commun.* 1996, 2527.
- [5] L. S. Hollis, W. I. Sundquist, J. N. Burstyn, W. J. Heigerberns, S. F. Bellon, K. J. Ahmed, A. R. Amundsen, E. W. Stern, S. J. Lippard, *Cancer Res.* 1991, 51, 1866.
- [6] Y. Zou, B. Van Houten, N. Farrell, *Biochemistry* 1993, 32, 9632.
- [7] B. A. Murrer, Eur. Patent Appl. EP 0727430 A1, Bulletin 34, 1996.
- [8] F. Raynaud, F. Boxall, P. Goddard, M. Valenti, M. Jones, B. Murrer, C. Giandomenico, L. Kelland, *Proc. 88th Annual Meeting American Assoc. Cancer Res.*, April 12–16, 1997, San Diego, CA, Vol. 38, No. 2085, pp. 311.
- [9] S. J. S. Kerrison, P. J. Sadler, *J. Chem. Soc. Chem. Commun.* 1977, 861.
- [10] S. J. Barton, K. J. Barnham, A. Habtemariam, P. J. Sadler, R. E. Sue, *Inorg. Chim. Acta*, in press.
- [11] M. Piotta, V. Saudek, V. Sklenar, *J. Biomol. NMR* 1992, 2, 661.
- [12] J. Stonehouse, G. L. Shaw, J. Keeler, E. D. Laue, *J. Magn. Reson. Ser. A* 1994, 107, 178.
- [13] P. Colamarino, P. L. Orioli, *J. Chem. Soc. Dalton Trans.* 1975, 1656.
- [14] G. H. W. Milburn, M. R. Truter, *J. Chem. Soc. (A)* 1966, 1609.
- [15] E. G. Talman, W. Brüning, J. Reedijk, A. L. Spek, N. Veldman, *Inorg. Chem.* 1997, 36, 854.
- [16] S. J. Berners-Price, P. J. Sadler, *Coord. Chem. Rev.* 1996, 151, 1.
- [17] G. Pettit, L. D. Pettit, *IUPAC Stability Constants Database*, IUPAC and Academic Software, Otley (UK), 1993.
- [18] S. E. Miller, D. A. House, *Inorg. Chim. Acta* 1989, 161, 131.
- [19] F. Basolo, J. Chatt, H. B. Gray, R. G. Pearson, B. L. Shaw, *J. Chem. Soc.* 1961, 2207.
- [20] R. Romeo, D. Minniti, M. Trozzi, *Inorg. Chem.* 1976, 15, 1134.
- [21] A. F. LeRoy, R. T. Lutz, R. L. Dedrick, *Cancer Treatment Rep.* 1979, 63, 59.